Biotechnic & Histochemistry

ISSN: 1052-0295 (Print) 1473-7760 (Online) Journal homepage: https://www.tandfonline.com/loi/ibih20

Inhibiting effect of oleocanthal on neuroblastoma cancer cell proliferation in culture

Ülkün Ünlü Ünsal, Mesut Mete, Işil Aydemir, Yusuf Kurtuluş Duransoy, Ahmet Şükrü Umur & Mehmet Ibrahim Tuglu

To cite this article: Ülkün Ünlü Ünsal, Mesut Mete, Işil Aydemir, Yusuf Kurtuluş Duransoy, Ahmet Şükrü Umur & Mehmet Ibrahim Tuglu (2020) Inhibiting effect of oleocanthal on neuroblastoma cancer cell proliferation in culture, Biotechnic & Histochemistry, 95:3, 233-241, DOI: 10.1080/10520295.2019.1674919

To link to this article: https://doi.org/10.1080/10520295.2019.1674919

Published online: 06 Nov 2019.

BIOTECHNIC & HISTOCHEMISTRY
2020, VOL. 95, NO. 3, 233–241
https://doi.org/10.1080/10520295.2019.1674919

Taylor & Francis
Taylor & Francis Group

Inhibiting effect of oleocanthal on neuroblastoma cancer cell proliferation in culture

Ülkün Ünlü Ünsal [a], Mesut Mete[b], Işil Aydemir[c], Yusuf Kurtuluş Duransoy[b], Ahmet Şükrü Umur[b], and Mehmet Ibrahim Tuglu [d]

[a]Koc University School of Medicine Department of Neurosurgery, Istanbul, Turkey; [b]Manisa Celal Bayar University School of Medicine Neurosurgery Department, Manisa, Turkey; [c]Ömer Halisdemir University School of Medicine Histology-Embryology Department, Niğde, Turkey; [d]Manisa Celal Bayar University School of Medicine Histology-Embryology Department, Manisa, Turkey

ABSTRACT

We investigated the potential anticancer effects of oleocanthal (OC) on neuroblastoma cells. Cells were divided into four groups: group 1, neuroblastoma cells were treated with OC; group 2, neurons that differentiated from neuroblastoma cells were treated with phosphate-buffered saline(PBS); group 3, bone marrow derived neuronal (BMDN) cells that were differentiated from bone marrow derived mesenchymal stem cells (BMSCs) were treated with OC; group 4, BMDN cells that were differentiated from BMSCs were treated with PBS. Groups 2 and 4 were control groups. The effects of OC on cell viability, oxidative stress, neurite inhibition and apoptosis at IC_{50} dose were investigated using MTT analysis, i-NOS and e-NOS measurement, neurotoxicity screening test (NST) and TUNEL staining, respectively. MTT analysis demonstrated that cells were significantly less viable in group 1 than in group 3. i-NOS and e-NOS staining intensity was significantly greater in group 1 than in group 3. NST revealed that OC inhibited neurite growth in both neuroblastoma and BMND cells; inhibition was significantly less in group 3 than in group 1. Significantly more TUNEL labeled cells were found in group 1 than in group 3. We found that OC prevented growth and proliferation of neuroblastoma cells in culture by increasing oxidative stress and apoptosis. We also found that the cytotoxicity of OC is negligible in BMDN cells.

KEYWORDS

apoptosis; cancer; neuroblastoma; oleocanthal; stem cells

Neuroblastoma is an embryonal tumor that originates from precursor cells of the sympathetic nervous system. Twenty-five percent of neuroblastoma cases are congenital (Schroeder et al. 2009); sporadic cases are found in adolescents and adults. Neuroblastomas consist of small cells with a hyperchromatic nucleus and limited cytoplasm. Neuroblastoma cells in vivo often are separated from each other by thin fibrovascular septa. Homer Wright pseudorosettes can be found in 30% of cases. The most common genetic abnormality in neuroblastomas is N-myc amplification and deletion of the short arm of chromosome 1 (Kumar et al. 2005; Spitz et al. 2002). Approximately 30–50% of primary tumors with deletion of the short arm of chromosome 1 are associated with poor prognosis. Clinical signs and symptoms vary depending on the location of the primary tumor, metastasis or development of paraneoplastic syndrome. Treatment of neuroblastoma is difficult, costly and often unsuccesful (Goldsby and Matthay 2004; Kumar et al. 2005).

In Mediterranean countries, the lower incidence of cancer, neurodegenerative diseases and cardiovascular diseases compared to other European and Western countries appears to be associated with the Mediterranean diet (Khanfar et al. 2015) in which olive oil is a staple. Oleocanthal (OC) is a phenolic compound found in freshly pressed extra virgin olive oil. Beauchamp et al. (2005) reported that OC is responsible for the bitter aftertaste of olive oil leaves. These investigators also reported that OC inhibited COX-1 and COX-2 in a dose-dependent manner that resembled the anti-inflammatory effect of ibuprofen.

There are several reports of the inhibitory effect of OC on cancer and metastasis in vitro (Akl et al. 2014; Cusimano et al. 2017; Elnagar et al. 2011). These investigators reported a decrease in the proportion of lung, breast, prostate and gastrointestinal cancers in individuals that consume a Mediterranean diet compared to those that consume Western diets (Elnagar et al. 2011; Geula et al. 1998; Li et al. 2009; Pitt et al. 2009; Scotece et al. 2013). Although OC is

CONTACT Ülkün Ünlü Ünsal ulkununlu@hotmail.com Department of Neurosurgery, Koc University School of Medicine, Istanbul, urkey

a widely recognized phenolic with antioxidant activity, it has not been investigated adequately. Scotece et al. (2013) reported that OC exhibits antitumor activity by inhibiting macrophage inflammatory protein 1-alpha, which is responsible for osteolytic activity in multiple myeloma. Also, OC reduces the effects of two Hsp90 heat shock proteins, which stabilize proteins that participate in tumor growth (Margarucci et al. 2013).

We investigated the anticancer effects of OC on neuroblastoma cancer cells and neurons that are differentiated from BMDN stem cells by measuring oxidative stress and apoptosis.

Material and methods

Our study protocol was approved by the ethics committee of Celal Bayar University School of Medicine (No. 20.478.486). OC was obtained from Kale Naturel Chemical Co., Balıkesir, Turkey.

Experimental groups

We established groups of cells in culture. Group 1, neuroblastoma cells were treated with OC; group 2, neurons that differentiated from neuroblastoma cells were treated with phosphate-buffered saline (PBS); group 3, BMDN cells that were differentiated from BMSC were treated with OC; group 4, BMDN cells that were differentiated from BMSC were treated with PBS. We replaced OC with the same amount of PBS for the control groups, groups 2 and 4. We investigated the effects of OC on cell viability, oxidative stress, inhibition of neurites and apoptosis at IC_{50} dose using 3-[4.5-dimethylthiazol-2-yl]-2.5- diphenyltetrazolium bromide (MTT) analysis, immunocytochemical staining of inducible nitric oxide synthase (i-NOS) and endothelial nitric oxide synthase(e-NOS), neurotoxicity screening test (NST) and terminal deoxynucleotidyl transferase-mediated dUTP nick end-labeled (TUNEL) staining, respectively.

Culture of NB2a cells

NB2a mouse neuroblastoma cell line was purchased from Republic of Turkey Ministry of Food Agriculture and Livestock, Şap Instıtute, Ankara, Turkey. Cells were grown in Dulbecco's modified Eagle medium (DMEM) containing 5% (v/v) horse serum, 5% (v/v) fetal bovine serum (FBS), 200 mM L-glutamine, 100 U/ml penicillin, 100 µg/ml streptomycin and 25 µg/ml gentamicin; all reagents were purchased from Biochrom (Berlin, Germany). The cells were maintained in culture flasks in a humidified incubator at 37 °C and 5% CO_2. The medium was changed every two days (Vural and Tuğlu 2011).

Isolation of bone marrow derived mesenchymal stem cells (BMSCs)

BMSCs were obtained from the tibias of a 250 g male Wistar rat and cultured in alpha-minimum essential medium (α-MEM) containing 15% fetal calf serum (FCS), 50 µg/ml gentamycin, 100 U/ml penicillin, 100 UI/ml streptomycin and 100 U/ml amphotericin, all from Biochrom. Briefly, bones were excised aseptically from the hindlimbs of the rat following ether euthanasia. The soft tissue was removed and both tibias were cut with sterile scissors, a hole was created in each bone with an 18 gauge needle and the marrow was flushed from the shaft into medium without supplements. Cells were maintained at 37 °C and 5% CO_2 for 3 days, after which the medium was replaced with fresh medium supplemented with FCS to remove nonadhering cells. Attached cells then were grown to confluence and passaged until passage 3 (P3) Mete et al. (2016).

Neuronal differentiation of NB2a and BMSCs

NB2a cells and BMSCs were placed in 24-well plates at a density of 15 x 10^3 cells/well and allowed to grow for 24 h. The culture medium was replaced with serum-free medium containing 20 µl epidermal growth factor (EGF) and 20 µl fibroblast growth factor (FGF) for neuronal differentiation. Neurite outgrowth and neuronal differentiation were observed using phase contrast microscopy. At the end of day 7, cells were stained immunocytochemically for neuronal differentiation markers, nestin and tubulin; for glial fibrillary acidic protein (GFAP) for astrocytes; and oligodendrocyte marker, O4, for oligodendrocytes using a mouse rat neural stem cell functional identification kit SC013 (R&D Systems, Minneapolis, MN) according to the manufacturer's instructions (Mete et al. 2016).

Determination of cytotoxicity

MTT analysis (M6494; Invitrogen Camarillo, CA) assay was used to determine possible toxicity of OC. After neuronal differentiation, cells were seeded into 96-well plates and exposed to 0, 0.1, 1, 10, 100 and 1000 µM OC for 24 h. After 24 h, the medium with OC was removed and 100 µl fresh medium without FCS supplementation was placed in each well and 10 µl 12 mM MTT stock solution was added and incubated

for 4 h at 37 °C in a 5% CO_2 humidified incubator. Medium containing MTT was decanted and cells were incubated with 50 µl dimethylsulfoxide (DMSO) (A3672; Sigma; Darmstadt, Germany) for 10 min at room temperature, then the absorbance was read at 570 nm using a UV-visible spectrophotometer multiplate reader (ELx800UV; BioTek, Überlingen, Germany) and IC_{50} doses of OC were calculated for each group. Experiments were repeated three times and data are presented as means ± SD (Pitt et al. 2009).

NST assay

For NST, cells were exposed to IC_{50} doses of OC for 24 h. Cells then were fixed in 4% formaldehyde for 10 min, rinsed in PBS and stained with 0.6% Coomassie blue for 3 min. Cells were washed three times with PBS and photographed using an Olympus BX40 light microscope (Olympus, Tokyo, Japan) with a video camera (JVC-TK-C 601; Olympus) for digital imaging. Images were analyzed using an Image-Pro Plus image analyzer (5.1.259; Bioscience Technology, Bethesda, MD). Ten fields that contained approximately 10 cells each were selected for measurement for each group. A software algorithm was designed using the image analyzer functions of the microscope to enable automatic measurement of total neurite length in pixels for the cells in a given field and to express the results as the average neurite length/cell (Scotece et al. 2013).

Immunocytochemistry

Cells were immunostained for e-NOS and i-NOS to evaluate levels of oxidative stress. After application of OC at IC_{50} dose, the cells were fixed in 4% paraformaldehyde for 30 min and washed in PBS three times for 5 min each. Permeabilization was performed using 0.1% Triton X-100 (A4975; AppliChem, Darmstadt, Germany) at 4 °C for 15 min and cells were washed with PBS. Endogenous peroxidase activity was inhibited using 3% hydrogen peroxide for 5 min. Cells were washed with PBS and incubated with anti-eNOS rabbit polyclonal antibody (RB-1711-P1; Neomarkers, Fremont, CA) diluted 1:100 and anti-i-NOS rabbit polyclonal antibody (RB-1605-P; Neomarkers) diluted 1:100 for 18 h at 4 °C. The cells were washed three times for 5 min each in PBS, treated with biotin-streptavidin hydrogen peroxidase secondary antibody (Invitrogen-Histostain Plus Bulk Kit®, 85-9043; Invitrogen) for 30 min. After washing with PBS three times for 5 min each, cells were incubated with diaminobenzidine (DAB) (00-2020; Zymed, Burlingame CA) for 5 min for immunolabeling, then counterstained with Mayer's hematoxylin (72804E; Microm, Walldorf, Germany). Cells were covered with mounting medium (AML060; Scytek, Logan, UT) and photographed using an Olympus light microscope (BX40; Tokyo, Japan). Control samples were processed identically except that the primary antibody was omitted. The immunostaining was repeated three times.

Immunostaining intensity was scored by two blinded observers as 0, no staining; 1, weak staining; 2, moderate staining; 3, moderate–strong staining; 4, strong staining; 5, very strong staining. The H-score then was calculated using the formula: H-score = Pi intensity of staining + 1, where Pi is the percentage of stained cells for each intensity varying from 0 to 100% (Mete et al. 2016).

TUNEL assay

To detect apoptosis, we used a Dead End Colorimetric TUNEL in situ apoptosis detection kit (Promega, Madison, WI) according to the manufacturer's instructions. The cells were fixed in 4% (w/v) paraformaldehyde for 30 min, then washed in PBS for 5 min. The cells were incubated with 20 µg/ml proteinase-K for 10 min, then rinsed in PBS. Endogenous peroxidase activity was inhibited by incubation with 3% hydrogen peroxide for 5 min followed by rinsing in PBS. Cells were treated with equilibration buffer for 5 min, then incubated with Tdt-enzyme for 60 min at 37 °C. TdT was omitted prior to the end reactions as the negative control. After Tdt treatment, cells were treated with 2 x SCC for 15 min, then washed three times in PBS for 5 min each. Streptavidin-peroxidase was applied for 45 min, then cells were rinsed in PBS. Apoptotic cells were labeled with diaminobenzidine (DAB) (00-2020; Zymed) and counterstained using Mayer's hematoxylin (72804E; Microm, Walldorf, Germany). Cells were washed in distilled water and mounted using aqueous medium. TUNEL staining was assessed by a blinded observer using an Olympus BX40 light microscope. To calculate apoptotic index, the TUNEL positive cells were counted in 10 areas and the following formula was used to determine percentage of labeled apoptotic cells: apoptotic index = (number of apoptotic cells/total number of cells) × 100 (Pourheydar et al. 2016).

Statistical analysis

The experiments were performed in triplicate. The results were calculated using GraphPad GraphPad

Software (San Diego, CA) using one-way ANOVA and presented as means ± SD. Statistical significance was defined as $p \leq 0.05$.

Results

The cytotoxicity of OC compared to PBS was determined for both NB2a and BMDN cells by MTT, immunocytochemistry, NST and TUNEL assays. NB2a and BMDN cells were photographed after culturing. NB2a exhibited a prominent nucleus and neurites. BMDN cells cultured with EGF and FGF and differentiated from BMSCs, also exhibited neurites. (Figures 1, 2). Neuronal differentiation of BMDN cells was verified by immunocytochemical staining of nestin, tubulin, GFAP and O4 before application of OC (Figure 3).

MTT was used to determine the IC_{50} dose of OC using PBS as control. The IC_{50} dose was calculated to be 100 µM for NB2a and 1,000 µM for BMDN cells (Figure 4). Cell viability was significantly less in group 1 than in group 3 ($p < 0.001$).

We used NST to determine neurite inhibition. OC inhibited neurite growth in both NB2a and BMDN cells. Neurite inhibition was greater in OC treated NB2a cells than in OC treated BMDN cells. Inhibition percentages were 51.44 ± 11.34 and 34.44 ± 8.78% for NB2a and BMDN cells, respectively; the difference between two groups was statistically significant ($p < 0.001$).

To understand better the mechanisms underlying the apparent antitumor effect of OC, cells were immunostained for oxidative stress markers, e-NOS and i-NOS. The H-scores are given in Figure 5. The immunoreactivity of e-NOS was increased in the OC treated NB2a cells compared to untreated cells. Also, application of OC to BMDN cells increased the immunoreactivity of e-NOS. Application of OC increased the immunoreactivity of i-NOS in both NB2a and BMDN cells ($p < 0.001$). Both e-NOS and i-NOS staining was significantly greater in OC treated

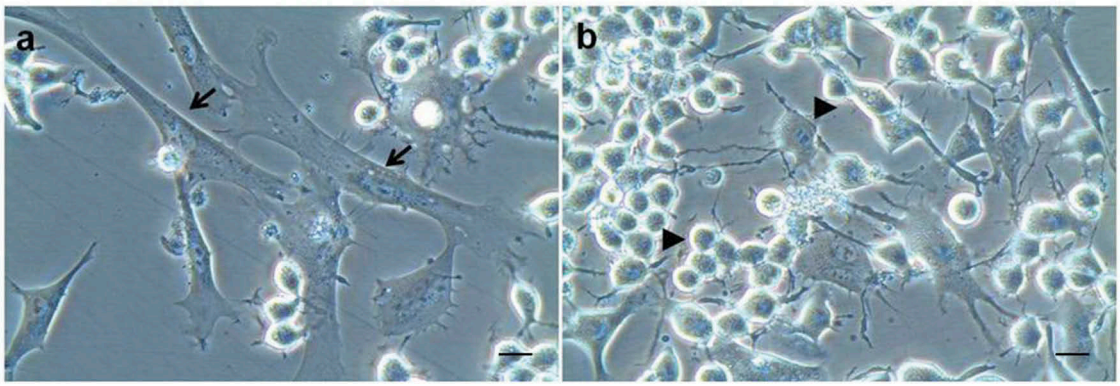

Figure 1. Differentiation of BMSCs into neurons. a) Early differentiation. b) Late differentiation. Arrows, mesenchymal stem cells; arrowheads, neurons.

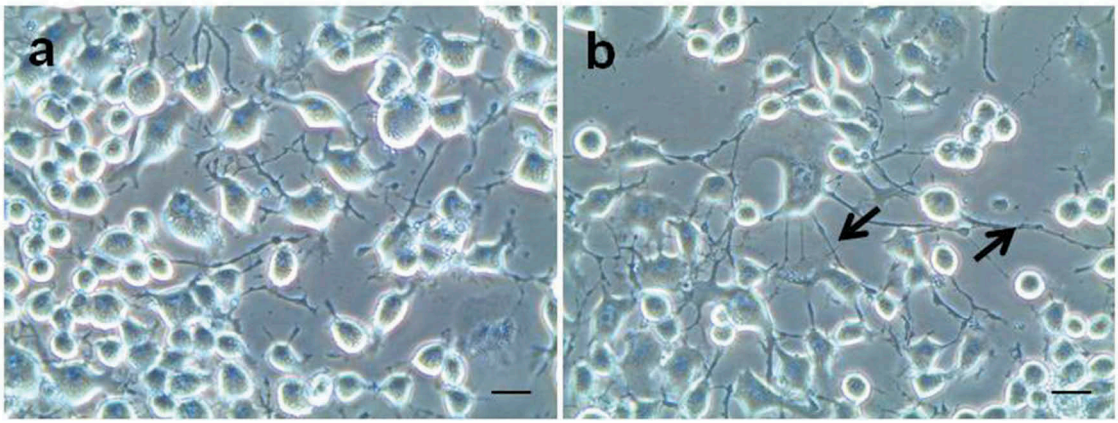

Figure 2. Differentiation of NB2a mouse neuroblastoma cells into neurons. a) Early differentiation. b) Late differentiation, neurons. Arrows, neurites.

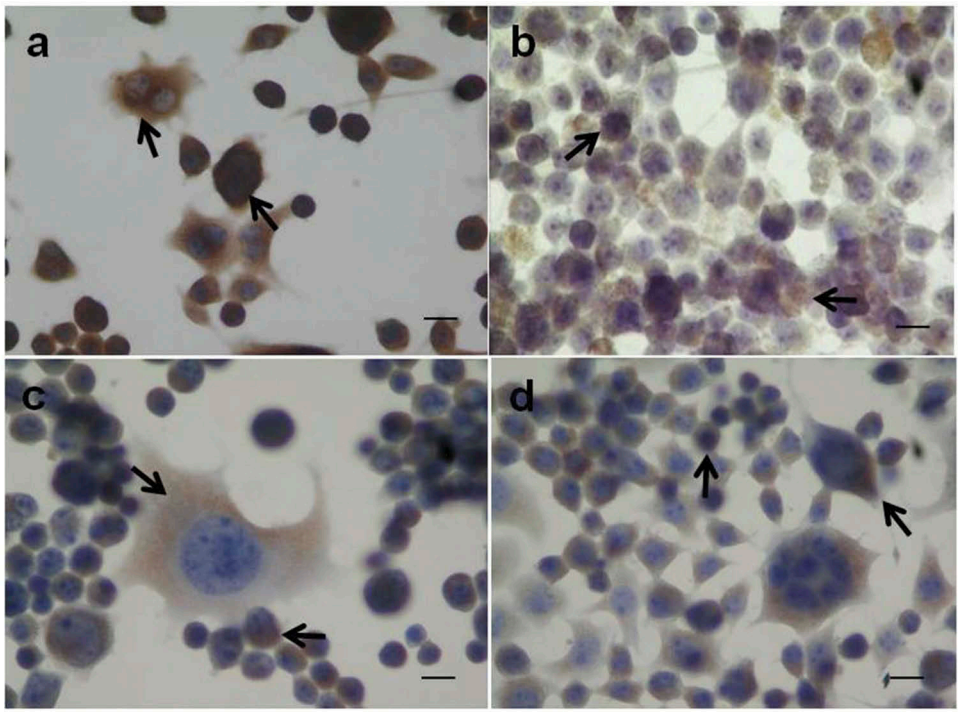

Figure 3. Characterization of neurons differentiated from BMSCs by immunocytochemistry using nestin (a), tubulin (b), GFAP (c) and oligodendrocyte-4 (d) markers. Primary culture of BMDN expressed mostly nestin and tubulin and scarely expressed GFAP and oligodendrocyte-4. These expressions of markers changed to neural markers only at pasage 3. Scale bars = 20 µm.

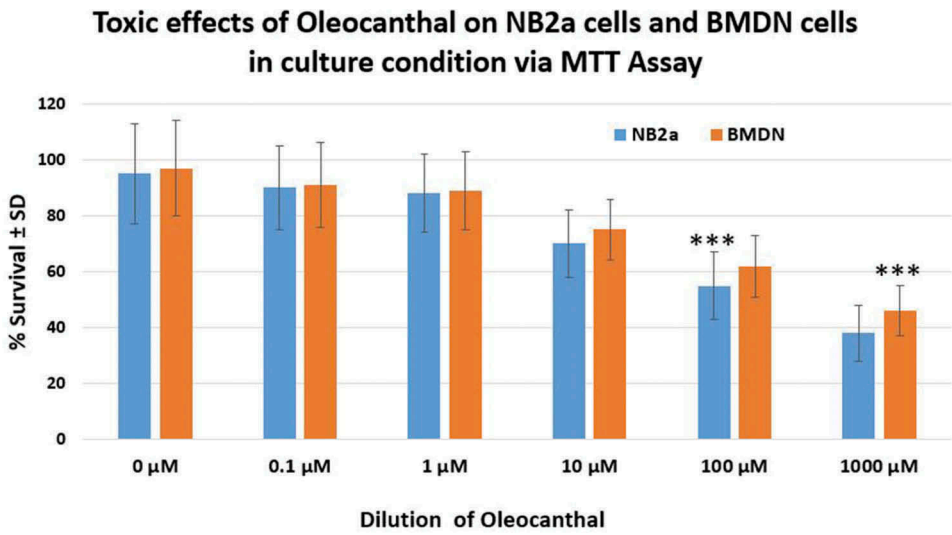

Figure 4. MTT analysis showed the toxic effect of OC on NB2a and BMDN cells. The toxic effect was less in BMDN cells and this difference was statistically significant at 1 µM compared to 100 µM (***$p < 0.001$). This toxic effect was greater for NB2a cells at IC_{50} 100 µM dose than for BMDN cells (*$p < 0.05$).

NB2a cells than in OC treated BMDN cells ($p < 0.001$) (Figures 6, 7).

We used TUNEL staining to evaluate apoptosis. The number of apoptotic cells increased with application of OC to both NB2a and BMDN cells compared to control groups. We found that the toxic effect of OC was significantly greater than for the control groups. Also, we found that apoptosis was more common in the NB2a cells than BMDN cells ($p < 0.05$) (Figure 8).

Discussion

Neuroblastomas are responsible for approximately 15% of childhood cancer deaths. Surgery, radiotherapy and

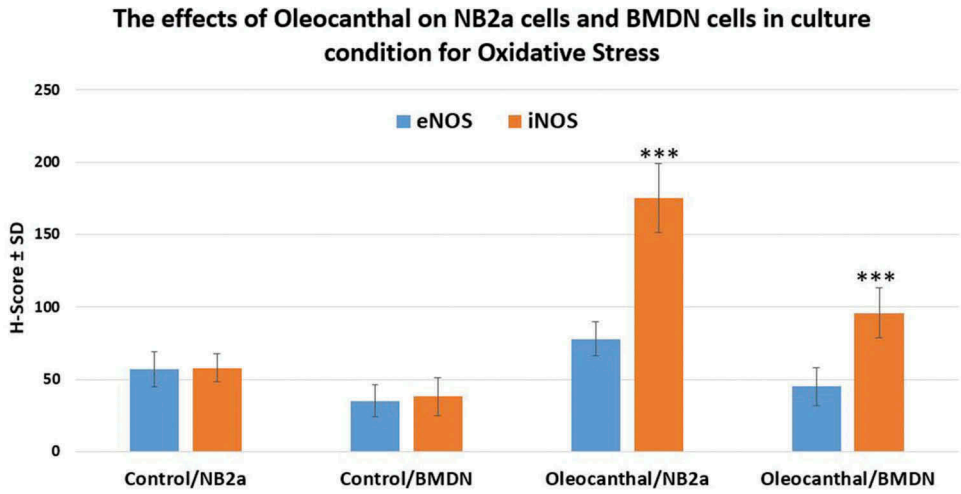

Figure 5. H-scores for control, NB2a and BMDN cells after application of OC. eNOS and i-NOS in NB2a cells were increased of after OC treatment. Both eNOS and i-NOS levels were higher in NB2a cells compared to BMDN cells.

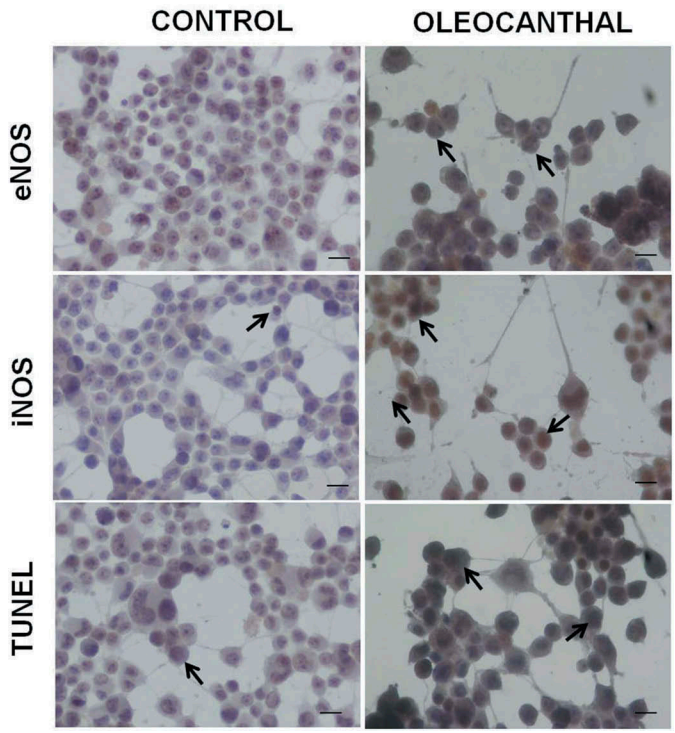

Figure 6. Immunocytochemical staining of eNOS, i-NOS and TUNEL in neurons from NB2a mouse neuroblastoma cells after application of OC. Labeled cells indicate apoptosis and oxidative stress in neurons. Scale bars = 20 μm.

chemotherapy are used to treat neuroblastoma. Unfortunately, recurrence is common with high resistance to therapy and usually results in death. Therefore, new treatment approaches are required (Schroeder et al. 2009; Gross et al. 1959). Like many other tumors, apoptosis is an important mechanism for arresting neuroblastoma. Neuroblastoma cells have been used as models for evaluating various anti-tumor approaches in vitro including arresting cell cycle, inducing apoptosis and decreasing N-myc expression (Li et al. 2017; Sharma et al. 2017; Takahashi et al. 2017).

OC is a phenolic component of extra virgin olive oil. OC has been shown in vitro to exhibit inhibition of COX-1 and COX-2 and activation of adenosine monophosphate activating protein via phosphorylated p53genes, which are associated with increased apoptosis (Beauchamp et al. 2005; Scotece et al. 2013). In addition, OC modifies the paired helical filaments-6 (PHF6) protein that inhibits tau-tau binding, which

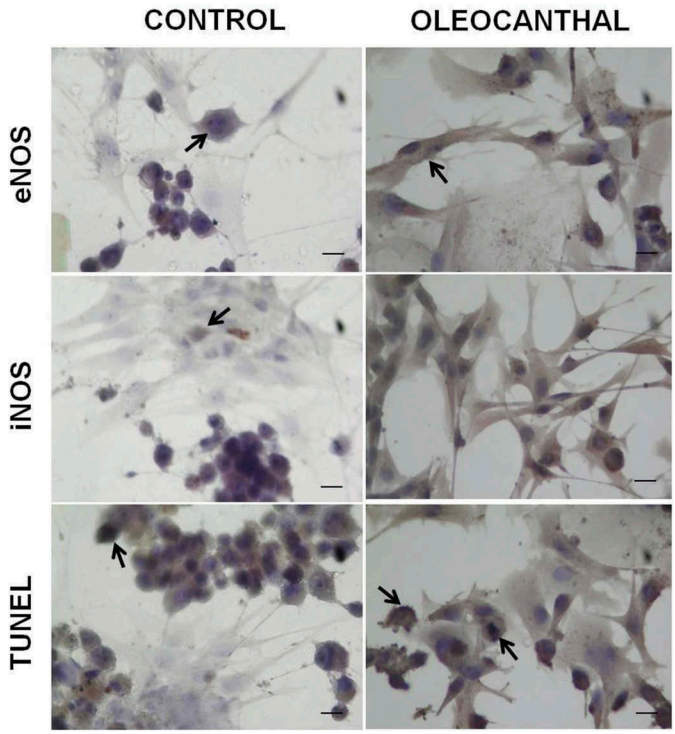

Figure 7. Immunocytochemical staining of eNOS, i-NOS and TUNEL in neurons from BMSCs after application of OC. Labeled cells indicate apoptosis and oxidative stress in neurons. Scale bars = 20 μm.

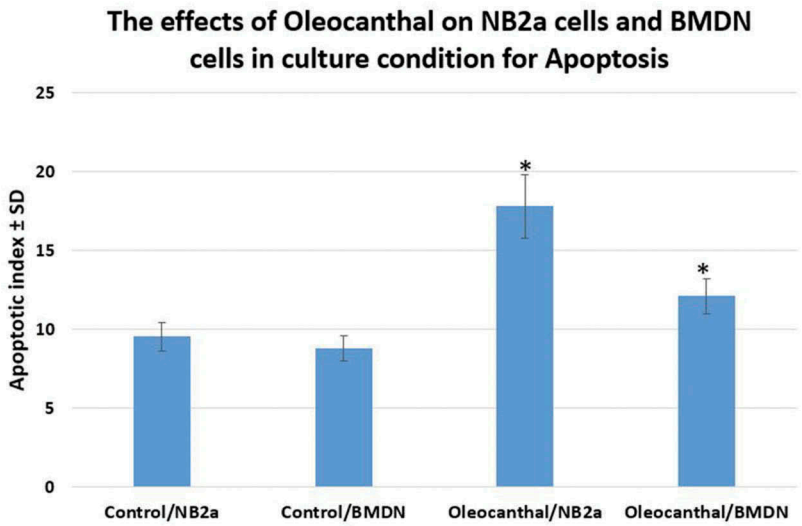

Figure 8. Apoptotic index (TUNEL) analysis of control, NB2a and BMDN cells after application of OC. Note increasing level of apoptosis in NB2a cells after OC treatment. Apoptosis was greater in NB2a cells compared to BMDN cells.

causes neuron degeneration. Therefore, OC might protect neurons from death by this mechanism (Li et al. 2009). The effects of OC have been investigated in vitro and in vivo for breast, prostate, multiple myeloma, gastrointestinal cancers and Alzheimer's disease (Elnagar et al. 2011; Li et al. 2009; Scotece et al. 2013). Scotece et al. (2013) reported that OC inhibits MIP-1α expression, and ERK1/2 and AKT signaling pathways, which lead to apoptosis in multiple myeloma cells. Akl et al. (2014) reported that OC inhibited the c-met dependent signaling pathway, which arrested the cell cycle at G1and caused apoptosis in breast cancer cells. Gu et al. (2017) reported that OC down-regulated STAT3 target genes including Mcl-1, Bcl-xL, MMP-2, MMP-9, VEGF, which participate in increasing apoptosis and decreasing invasion and

angiogenesis of melanoma. We found that OC suppressed proliferation and promoted apoptosis in neuroblastoma cells in vitro. We found also that TUNEL staining was significantly more prominent in OC treated NB2a cells than in OC treated BMDN cells.

High levels of reactive oxygen species (ROS) impair mitochondrial integrity and cause DNA damage. It is possible that malignant cells that exist under an increased level of oxidative stress could be more vulnerable to further increases of ROS. Therefore, the basal level of ROS might contribute to carcinogenesis and high levels of ROS might cause arrest of cancer cell growth, apoptosis or necrosis. The precise mechanism of apoptosis and oxidative stress is unclear (Cusimano et al. 2017; Gorrini et al. 2013). Cusimano et al. (2017) reported that OC treatment elicited expression of γH2AX, a marker for DNA damage, and increased intracellular ROS production and caused mitochondrial depolarization in a dose dependent manner. Also, OC inhibited cell viability and the colony formation capacity of hepatocellular carcinoma and colorectal carcinoma cells. Consistent with earlier reports, we found that OC affects neuroblastoma cancer cells in a dose-dependent manner. At the IC_{50} dose, cell viability, neurite inhibition and oxidative stress were more pronounced compared to control groups. MTT analysis revealed that cell viability in OC treated NB2a cells was significantly less than in OC treated BMDN cells. We found a significant increase in the immunoreactivity of i-NOS and e-NOS, which are used to evaluate oxidative stress, for OC treated NB2a and OC treated BMDN cells. The NST revealed that OC inhibited neurite outgrowth significantly compared to control groups in both groups of OC treated cells.

Neuronal differentiation of mesenchymal stem cells in vitro is induced by signaling pathways including mitogen-activated protein kinases (MAP)/extracellular signal-regulated kinases (ERK), retinoic acid, cyclic-adenosine-monophosphate (cAMP)/protein kinase A, hedgehog and bone morphogenetic proteins (BMP) signaling pathways (Bhaskar et al. 2014; Salehi et al. 2016). WNT5a signaling is initiated for neuronal differentiation in the presence of FGF (Rosso and Inestrosa 2013). EGF and FGF also can initiate neuronal differentiation via the MAPK/ERK pathway (Cargnello and Roux 2011; Park et al. 2011). We used the combination of EGF and FGF for neuronal differentiation for both NB2a and BMSC cells. Therefore, we could compare the toxicity of OC in neurons that differentiated from NB2a and BMSC cells. Our results showed that OC toxicity was greater for NB2a cells than for BMDN cells.

We demonstrated the apoptotic effect of OC on neuroblastoma cancer cells using the TUNEL method. OC proved to be an effective anticancer drug due to its ability to kill cancer cells without affecting normal cells. Our findings indicate the potential of OC for treatment of neuroblastoma and may provide a basis for future investigation of its use in humans.

Acknowledgments

Ülkün Ünlü Ünsal and Mesut Mete contributed equally to the writing of this article. This study was presented as an oral presentation at the Scientific Congresses of Turkish Neurosurgical Society.

Declaratıon of ınterest

The authors report no conflicts of interest. The authors alone are responsible for the content and writing of this paper.

ORCID

Ülkün Ünlü Ünsal http://orcid.org/0000-0001-5194-3138
Mehmet Ibrahim Tuglu http://orcid.org/0000-0002-0569-8415

References

Akl MR, Ayoub NM, Mohyeldin MM, Busnena BA, Foudah AI, Liu YY, Sayed KA. (2014). Olive phenolics as c-Met inhibitors: oleocanthal attenuates cell proliferation, invasiveness, and tumor growth in breast cancer models. PLoS One. 21; 95:e97622.

Beauchamp GK, Keast RSJ, Morel D, Lin J, Pika J, Han, Q, Lee CH, Smith AB, Breslin PAS. (2005). Phytochemistry: ibuprofen-like activity in extra-virgin olive oil. Nature. 437:45–46.

Bhaskar B, Mekala NK, Baadhe RR, Rao PS. (2014). Role of signaling pathways in mesenchymal stem cell differentiation. Curr Stem Cell Res Ther. 96:508–512.

Cargnello M, Roux PP. (2011). Activation and function of the MAPKs and their substrates, the MAPK-activated protein kinases. Microbiol Mol Biol Rev. 751:50–83.

Cusimano A, Balasus D, Azzolina A, Augello G, Emma MR, Di Sano C, Gramignoli R, Strom SC, McCubrey JA, Montalto G, Cervello M. (2017). Oleocanthal exerts antitumor effects on human liver and colon cancer cells through ROS generation. Int J Oncol. 512:533–544.

Elnagar AY, Sylvester PW, El Sayed KA. (2011) Oleocanthal as a c-Met inhibitor for the control of metastatic breast and prostate cancers. Planta Med. 77:1013–1019.

Geula C, Wu CK, Saroff D, Lorenzo A, Yuan M, Yankner BA. (1998) Aging renders the brain vulnerable to amyloid beta-protein neurotoxicity. Nat Med. 47:827–831.

Goldsby RE, Matthay KK. (2004). Neuroblastoma: evolving therapies for a disease with many faces. Ped Drugs. 62:107–122.

Gorrini C, Harris IS,Mak TW. (2013). Modulation of oxidative stress as an anticancer strategy. Nat Rev Drug Discov. 12:931–947.

Gross RE, Farber S, Martin LW. (1959) Neuroblastoma sympatheticum: a study and report of 217 cases. Pediatrics. 23:1179–1191.

Gu Y, Wang J, Peng L. (2017). (-)-Oleocanthal exerts anti-melanoma activities and inhibits STAT3 signaling pathway. Oncol Rep. 371:483–491.

Khanfar MA, Bardaweel SK, Akl MR, El Sayed KA. (2015) Olive oil-derived oleocanthal as potent ınhibitor of mammalian target of rapamycin: biological evaluation and molecular modeling studies. Phytother Res. 2911:1776–1782.

Kumar V, Abbas AK, Fausto N. (2005). Robbins and Cotran pathologic basis of disease. 7th ed., Elsevier Saunders. Philadelphia, PA. p. 295–505.

Li W, Sperry JB, Crowe A, Trojanowski JQ, Smith AB, Lee VM. (2009). Inhibition of tau fibrillization by oleocanthal via reaction with the amino groups of tau. J. Neurochem. 110:1339–1351.

Li Y, Zhuo B, Yin Y, Han T, Li S, Li Z, Wang J. (2017) Anti-cancer effect of oncolytic adenovirus-armed shRNA targeting MYCN gene on doxorubicin-resistant neuroblastoma cells. Biochem Biophys Res Commun. 491:134–139 .

Margarucci L, Monti MC, Cassiano C, Mozzicafreddo M, Angeletti M, Riccio R, Tosco A, Casapullo A. (2013) Chemical proteomics-driven discovery of oleocanthal as an Hsp90 inhibitor. Chem Commun Camb. 49:5844–5846.

Mete M, Aydemir I, Ünsal ÜÜ, Duransoy YK, Tuğlu Mİ, Selçuki M. (2016). Neuroprotective effects of bone marrow-derived mesenchymal stem cells and conditioned medium in mechanically injured neuroblastoma cells. Turk J Med Sci. 46:1900–1907.

Park S, Jung HH, Park YH, Ahn JS, Im YH. (2011) ERK/MAPK pathways play critical roles in EGFR ligands-induced MMP1 expression. Biochem Biophys Res Commun. 407:680–686.

Pitt J, Roth W, Lacor P, Smith AB 3rd, Blankenship M, Velasco P, De Felice F, Breslin P, Klein WL. (2009) Alzheimer's-associated abeta oligomers show altered structure, immunoreactivity and synaptotoxicity with low doses of oleocanthal. Toxicol Appl Pharmacol. 2402:189–197.

Pourheydar B, Soleimani Asl S, Azimzadeh M, Rezaei Moghadam A, Marzban A, Mehdizadeh M. (2016) Neuroprotective effects of bone marrow mesenchymal stem cells on bilateral common carotid arteries occlusion model of cerebral ischemia in rat. Behav Neurol. 2016:2964712. Epub 2016 Oct 25.

Rosso SB, Inestrosa NC. (2013). WNT signaling in neuronal maturation and synaptogenesis. Front Cell Neurosci. 7:103.1–11. doi:10.3389/fncel.2013.00103.

Salehi H, Amirpour N, Niapour A, Razavi S. (2016). An overview of neural differentiation potential of human adipose derived stem cells. Stem Cell Rev. 121:26–41.

Schroeder H, Wacher J, Larsson H, Rosthoej S, Rechnitzer C, Petersen BL, Carlsen NL. (2009). Unchanged incidence and increased survival in children with neuroblastoma in Denmark 1981-2000: a population-based study. Br J Cancer. 100:853–857.

Scotece M, Gomez R, Conde J, Lopez V, Gomez Rein J, Lago F, Smith AB 3rd, Gualillo O. (2013). Oleocanthal inhibits proliferation and MIP-1a expression in human multiple myeloma cells. Curr Med Chem. 20:2467–2475.

Sharma RK, Candelario-Jalil E, Feineis D, Bringmann G, Fiebich BL, Akundi RS. (2017). 1-Trichloromethyl-1,2,3,4-tetrahydro-beta-carboline TaClo) alters cell cycle progression in human neuroblastoma cell lines. Neurotox Res. 324:649–660.

Spitz R, Hero B, Westermann F, Ernestus K, Schwab M, Berthold F. (2002) Fluorescence in situ hybridization analyses of chromosome band 1p36 in neuroblastoma detect two classes of alterations. Genes Chrom Cancer. 343:299–305.

Takahashi N, Koyama S, Hasegawa S, Yamasaki M, Imai M. (2017) Anticancer efficacy of p-dodecylaminophenol against high-risk and refractory neuroblastoma cells in vitro and in vivo. Bioorg Med Chem Lett. 27:4664–4672.

Vural K, Tuğlu MI. (2011) Neurotoxic effect of statins on mouse neuroblastoma NB2a cell line. Eur Rev Med Pharmacol Sci.159:985–991.